Title

Biomimetic Ant-Nest Electrode Structures for High Sulfur Ratio Lithium—Sulfur Batteries

Journal

Nano Letters, 16(9)

ISSN

1530-6984

Authors

Ai, Guo

Dai, Yiling

Mao, Wenfeng

et al.

Publication Date

2016-09-14

DOI

10.1021/acs.nanolett.6b01434

Peer reviewed

Biomimetic Ant-Nest Electrode Structures for High Sulfur Ratio Lithium-Sulfur Batteries

Guo Ai[a, b], Yiling Dai[a], Wenfeng Mao[a], Hui Zhao[a], Yanbao Fu[a], Xiangyun Song[a], Yunfei En[b], Vincent S. Battaglia[a], Venkat Srinivasan[a], Gao Liu[a]*

[a]*Energy Storage and Distributed Resources Division, Energy Technologies Area, Lawrence Berkeley National Laboratory, Berkeley, California 94720, United States*

[b]*Science and Technology on Reliability Physics and Application of Electronic Component Laboratory, No. 5 Electronic Research Institute of the Ministry of Industry and Information Technology, Guangzhou 510610, China*

[*] *Corresponding author: Gao Liu, Tel.: +1-510-486-7207; Email: gliu@lbl.gov*

Abstract

The lithium-sulfur (Li-S) rechargeable battery has the benefit of high gravimetric energy density and low cost.,Significant research currently focuses on increasing the sulfur loading and sulfur/inactive-materials ratio, to improve life and capacity. Inspired by nature's ant-nest structure, this research results in a novel Li-S electrode that is designed to meet both goals. With only three simple manufacturing-friendly steps, which include slurry ball-milling, doctor-blade-based laminate casting, and the use of the sacrificial method with water to dissolve away table salt, the ant-nest design has been successfully re-created in an Li-S electrode. The efficient capabilities of ant-nest structure are adopted to facilitate fast ion transportation, sustain polysulfide dissolution, and assist efficient precipitation. High cycling stability in the Li-S batteries, for practical applications, has been achieved with up to 3 $mgcm^{-2}$ sulfur loading. Li-S

electrodes with up to 85% sulfur ratio have also been achieved for the efficient design of this novel ant-nest structure.

High energy density and low cost rechargeable batteries are attracting great interest because of increasing manufacturing and consumer demand for portable devices, electric vehicles and stationary energy storage systems that have longer charge times and overall battery lives[1-4]. The lithium-sulfur (Li-S) battery is one of the most promising candidates because of its high energy density (2600 $Whkg^{-1}$), environmental friendliness, and low cost due to the earth-abundant resource of elemental sulfur—which is also a by-product from the petroleum industry[5-8]. However, the application of Li-S batteries has been hindered by several shortcomings, including poor cycling stability, low coulombic efficiency, and practical low energy density at the cell level. These shortcomings primarily stem from the dissolution of polysulfide in the electrolyte as an intermediate species during both charge and discharge processes. The polysulfide could diffuse to and react with Li-metal electrode through the shuttle effect, resulting in active material loss and self-discharge[9-11]. A significant amount of research has addressed this issue, which includes studies and work to encapsulate the polysulfide with well-designed structure[12,13], attract polysulfide through functional groups with strong affinity[14-18], and eliminate polysulfide dissolution with the design of an electrolyte additive[19,20]. Another issue that limits the performance of Li-S batteries is the poor electrical conductivity of the reaction products (S_8 in the charged state and Li_2S/Li_2S_2 in the discharged state), which is also an obstacle to the high utilization of the active material[21]. In most research work, conductive additives with high weight ratio (40%–50%) are incorporated into the electrode to solve this problem, and a complicated design of sulfur/carbon composites needs to be performed. Therefore, the active material (sulfur) content is low at the electrode level, and practical energy density of the Li-S batteries suffers[22]. The next step in advancing Li-S technology is to design a high-efficiency Li-S electrode that can

achieve high practical energy density, have good cycling stability, and minimize the composition of the inactive component (e.g., conductive additive, binder, current collector, etc.).

To achieve these application goals, additional high-loading Li-S battery research is critical as well as intriguing to the research community. In the effort to maximize energy density in Li-S batteries, especially in high-power applications (e.g., high current output), the most predominant issue is blocking ion transportation channels[22,23]. In high-loading Li-S batteries, a significant amount of solid sulfur species (S_8 in the charged state and Li_2S/Li_2S_2 in the discharged state) will precipitate on the electrode/electrolyte interface during charge/discharge process[24-26]. Since they are highly insulating, the ion transportation channels in electrodes are likely to be blocked, which will result in poor sulfur utilization and severe shuttle effect. Another critical issue for high loading Li-S batteries is that larger amounts of polysulfide dissolution lead to much more severe shuttle effect. Therefore, the ability of the electrode to sustain the polysulfide well becomes a key issue. Also, mechanical issues arise as the electrode becomes thicker to increase area loading. Cracks and delamination in the electrode are common if the binder can't carry the inner stress[22]. Therefore, to achieve a high-efficiency, high-loading Li-S battery, several properties of the Li-S design need to be addressed: first, enough interconnected and continuous open channels to facilitate fast Li-ion and polysulfide transportation; secondly, highly conductive surface for polysulfide reaction and S_8 or Li_2S/Li_2S_2 precipitation; thirdly, the capability of the electrode to retain polysulfide and mitigate their diffusion into the electrolyte.

To address these concerns, this research team integrated all the design criteria, and proposed a novel and highly efficient electrode structure for Li-S batteries in this work. The structure is inspired by nature's own super-efficient ant-nest. The structure of the ant-nest network is famous for the smart spacial design with abundant storage space and multi interconnected channels

between storage sites, which allows for efficient and fast transportation of food[27]. The novel ant-nest electrode is fabricated using cost-effective industry-scale processing methods: ball-milling for slurry mixing, the doctor-blade method for laminate casting, and feasible sacrificial method for porous creation. Multiwall carbon nanotube (CNT), known as the world's best conductive agent [28], is selected for the conductive additive to enable ultra-fast and long-distance electron transportation. Also, the large surface area of CNT can provide increased reaction interface S species precipitation. Table salt (sodium chloride, NaCl), which costs little and is abundant and environmental friendly, is selected as the sacrificial additive for the electrode design. After the laminate is casted, the NaCl micro-particles are removed from composite electrode by simple water washing. A perfect ant-nest structure in the Li-S electrode is formed using this simple method; its key characteristics include multi-interconnected channels for ultra-fast Li-ion transport, numerous micro/nano porous structures for sufficient polysulfide storage, and a large inner surface suitable for a reaction interface. With this structural design, the ant-nest electrode shows good performance at high sulfur loading up to 3 $mgcm^{-2}$ with 50wt% sulfur ratio (to the electrode).

Moreover, due to the fact that the large weight ratio of in-active material, usually as high as 40%–50%, will influence the energy density of Li-S batteries, current research suggests a critical need to create a Li-S battery with higher sulfur ratio[22,29]. Research efforts pursuing this goal have had limited success[30,31]. In this team's work, using the ant-nest structure Li-S electrode, sulfur composition can be pushed up to 85wt%, with only 12wt% CNT and 3wt% binder at electrode scale. A practical energy density as high as $509mWhg^{-1}$ can be achieved, calculated at cell level. This research demonstrates the potential of this ant-nest electrode via successful high loading and high sulfur ratio Li-S systems, and is offered as an advancement in Li-S battery technology.

Transport channel blocking issue for the high-loading Li-S batteries. Fast ion transport capability is the most crucial factor for high-loading Li-S batteries. But in most cases the transport is not sufficient due to the liable blocking of the transport channels and limited reaction surface, especially in the case of high rate requirement. This will lead to low cycling capacity and poor sulfur utilization[22]. In this work, the phenomena is demonstrated via two Li-S electrode systems using CNT and acetylene black (AB) as conductive additives at different sulfur loading, respectively. For Li-S cells with the CNT additive, named CNT-S, two different sulfur loadings of 1.78 $mgcm^{-2}$ and 3.17 $mgcm^{-2}$ are tested, shown in Fig. 1(a-b). Low actual capacity and sulfur utilization are observed in both cells, especially at C/3 and higher loading, and the area capacity for two cells is very similar, being below 1$mAhcm^{-2}$, in Fig. S1(a). The main reason for this issue can be analyzed via the voltage profile, Fig. 1(b). In the 1.78 $mgcm^{-2}$ CNT-S cell, almost the same capacity is obtained from the upper voltage plateau both at C/10 and C/3, which corresponds to the long chain polysulfide dissolution (from S_8 to Li_2S_4); however, the capacity obtained from the lower voltage plateau shows a significant difference between C/10 and C/3. Only 200 $mAhg^{-1}$ capacity can be obtained at C/3 in this region, which is one quarter of the 800 $mAhg^{-1}$ obtained at C/10. This indicates that insufficient sulfur precipitation (from Li_2S_4 to Li_2S) exists in the second discharge plateau. This issue is more severe in Li-S electrodes with 3.17 $mgcm^{-2}$ sulfur loading, in which the lower plateaus are severely reduced both at C/10 and C/3. This demonstrates that the electrode structure can not support the simultaneous precipitation of a large quantity of polysulfide. This issue is also observed in different Li-S systems with acetylene black (AB) as additive (see Fig. S2).

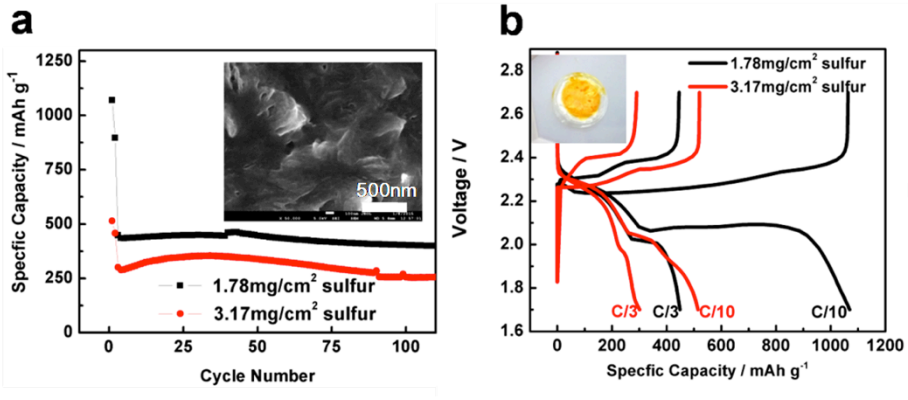

Figure 1. The cycling performance (a) and voltage profile (b) of the CNT-S cells with 1.78 mgcm^{-2} and 3.17 mgcm^{-2} sulfur loading. The SEM top morphology of the fully discharged CNT-S cell with 3.17 mgcm^{-2} sulfur loading is shown as an inset in figure 1(a), and a photo image of the separator of the same cell is shown in figure 1(b).

The main cause of this insufficient Li_2S precipitation is the blockage of the ion transport channel, which can be further elucidated via post-mortem analysis. A thick layer of Li_2S precipitation is observed on the ~3 mgcm^{-2} electrode after full discharge at C/3, shown in Fig. 1(a) inset, but the internal pores are still empty, as shown in Fig. S1. When current density is high, the sulfur species (Li_2S_x, x=1-2), which has a poor solubility and is highly insulating, is very likely to precipitate on the electrode surface next to the separator, blocking the small channels on the electrode surface. The electrode surface area is too small for efficient Li_2S precipitation. The thick Li_2S layer will lead to severe passivation of the electrode and early end of discharge, shown in Fig. 1(a). A large quantity of polysulfide will be blocked out and remain in the electrolyte, shown in Fig. 1(b) inset, which leads to low actual capacity. Once the surface pores and channels are blocked, no more charge/discharge can take place even with a further increase of the sulfur loading. Therefore, ion transport channel blockage and insufficient reaction interface have been the major limiting factor in further attempts to achieve high loading for Li-S batteries, both of which can be overcome by using the ant-nest structure that is proposed and designed in this work.

Simple method for ant-nest structure electrode design. In this work, the team integrates the above discussed criteria into the design of a novel ant-nest electrode structure for Li-S batteries (named as CNT-nest-S), which is designed to imitate nature's own ant-nest structure, taking advantage of its abundant storage and highly efficient transport system. The team adopts the common, cheap, abundant, and environmental friendly table salt (NaCl) as the sacrificial additive, which can be easily ball-milled down to smaller than 10μm. CNT, a well known and highly efficient carrier transport agent with ultra high carrier mobility, is selected as a conductive additive for the Li-S batteries in this work. The CNTs are interconnected to enable long distance charge transport and is able to process large surface areas. The salt is mixed directly with sulfur particles, binder, and CNT to form the slurry using the ball-milling method. After the laminate is casted, the NaCl micro-particles are removed from the composite electrode with a simple water washing, as shown in Fig. 2(a). A perfect ant-nest structure is formed with this simple method. The porous morphology of the ant-nest electrode structure can be demonstrated with the electrode cross-section and surface SEM morphology, as shown in Fig. 2(b-d). The micro size pores created by the templating NaCl crystals ensure numerous interconnected multi-ion channels, which both facilitate ion conduction and decrease the possibility of blockage by sulfur species precipitation. Both large and small pores exist in this ant-nest structure. The large micro-size pores generated by the templating NaCl particles for polysulfide storage and sustention. The nano-size pores between nanotubes, created by solvent evaporation are connected to the micro-pores, enabling the fully utilization of CNT surfaces. Therefore, the template approach has significantly enlarged the reaction interface in the electrode.

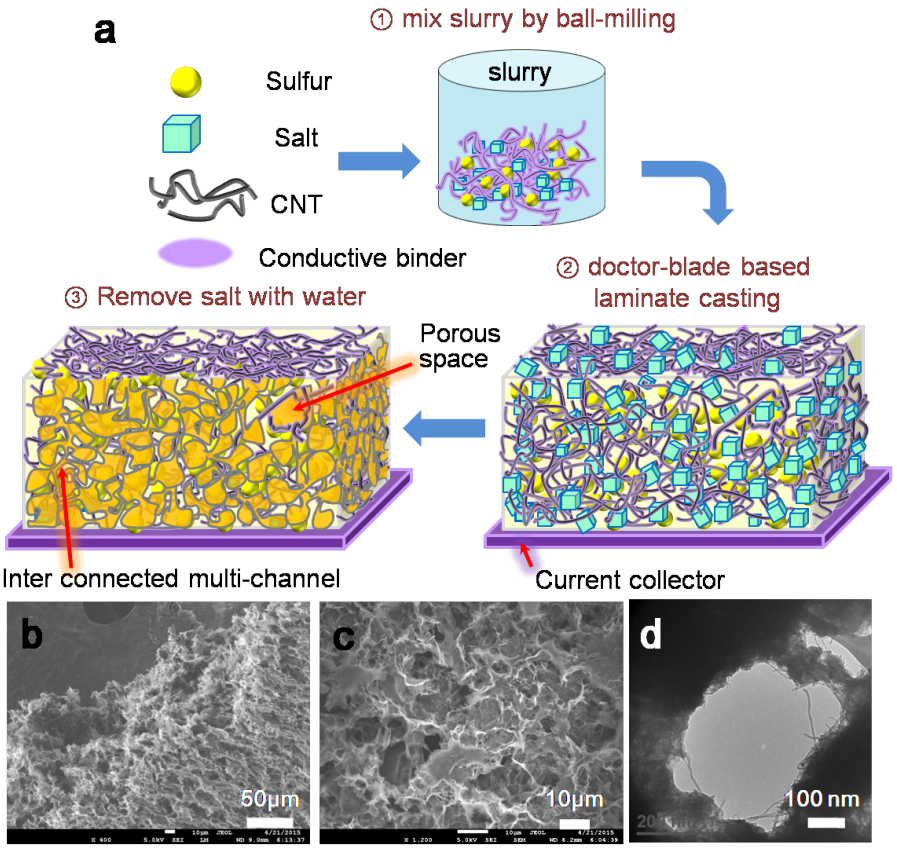

Figure 2. (a) Schematic illustration of the porous ant-nest structure Li-S electrode (CNT-nest-S) fabrication procedure. SEM cross-section (b) and top(c) morphology of CNT-nest-S. (d) The TEM morphology of the pore in the fully discharged CNT-nest-S.

The property of this structure meets all of the requirements for high loading Li-S batteries: (1) the interconnected channels between storage sites enable fast ion and polysulfide transport and prohibit channel blocking; (2) the nest structure features ample storage to efficiently sustain polysulfide as well as to accommodate sulfur volume change; (3) the maximized inner surface in the nest structure and the CNT facilitates efficient surface reaction for the transition among different sulfur species; (4) the functionalized conductive binder can help to further sustain the polysulfide inside storage pores with strong affinity between the functional binder and the polysulfide; (5) the conductive binder assists the interconnecting CNT framework in providing super conductivity and a long-distance charge transport pathway for the Li-S electrode; (6) the

strong mechanical properties of CNT and the binder enable the structure the mechanical strength to sustain the volume change during phase transformation of sulfur species. The ant-nest structure method is cost effective, facile, and allows for electrode-level fabrication, using only table salt and water as processing ingredients.

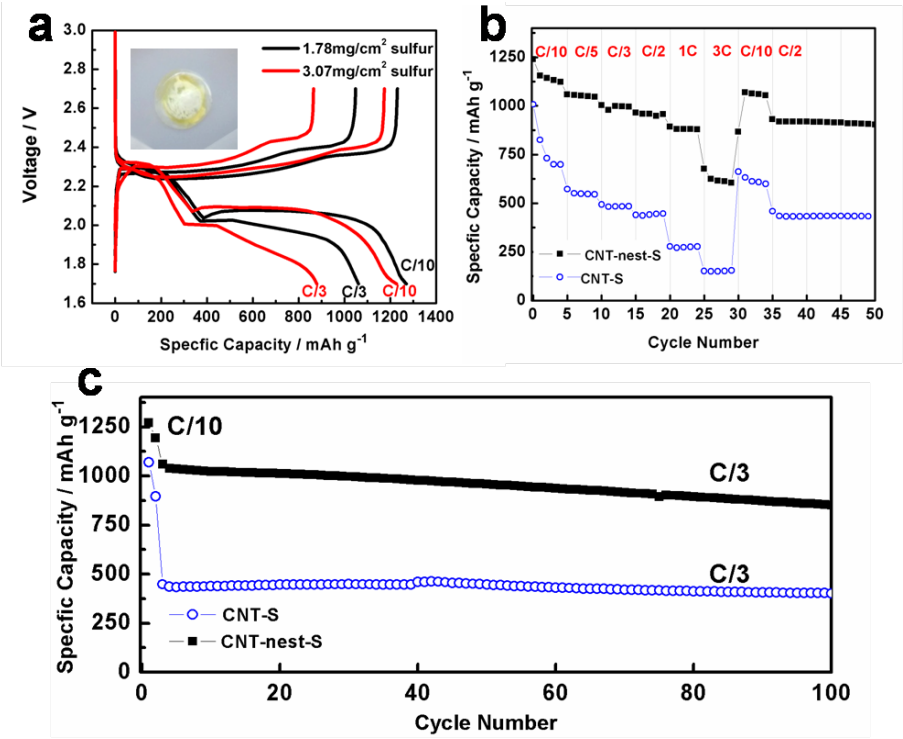

Figure 3. (a) The voltage profiles for the 1.78 mgcm^{-2} and 3.07 mgcm^{-2} CNT-nest-S cell at C/10 and C/3. The comparison of rate performance (b) and cycling performance (c) between CNT-S and CNT-nest-S cell, with sulfur loading 1.78 mgcm^{-2}.

Electrochemical characterization of the ant-nest Li-S electrode. The superior properties of the ant-nest structure can be demonstrated by examining its electrochemical performance, shown in Fig. 3(a-c). The two-plateau voltage profiles of CNT-nest-S cells of two loadings are similar both at C/10 and C/3, Fig. 3(a), indicating the CNT-nest-S structure enables good ion transporting as well as highly efficient sulfur dissolution (from S_8 to Li_2S_4) and precipitation

(from Li_2S_4 to Li_2S), without the channel blocking issue, even at 3.07 $mgcm^{-2}$ loading. Therefore, high sulfur utilization is achieved even at high rate discharge.

The comparison between the cells with (CNT-nest-S) and without (CNT-S) the nest structure further demonstrate the benefits of using the ant-nest structure. The CNT-nest-S electrode possesses superior cycling performance and rate performance over CNT-S, shown in Fig. 1 and Fig. 3. With the same charge and discharge rates, the specific capacity for CNT-nest-S structure from C/10 to 1C is quite similar, and a capacity of 615 $mAhg^{-1}$ can still be obtained at 3C. In contrast, less than half of the capacity is obtained at levels higher than C/5 in a regular CNT-S cell; less than 200 $mAhg^{-1}$ can be obtained at 3C. As a further indication of the properties of CNT-nest-S structure, long-term cycling performance at C/3 is plotted in Fig. 2(f). The stable cycling specific capacity of 1060 $mAhg^{-1}$ is achieved for the CNT-nest-S cell, but only 445 $mAhg^{-1}$ is achieve for CNT-S. These data gives strong evidence to the capabilities and potential of the CNT-nest-S structure in facilitating high loading Li-S batteries and achieving superior rate and cycling performance.

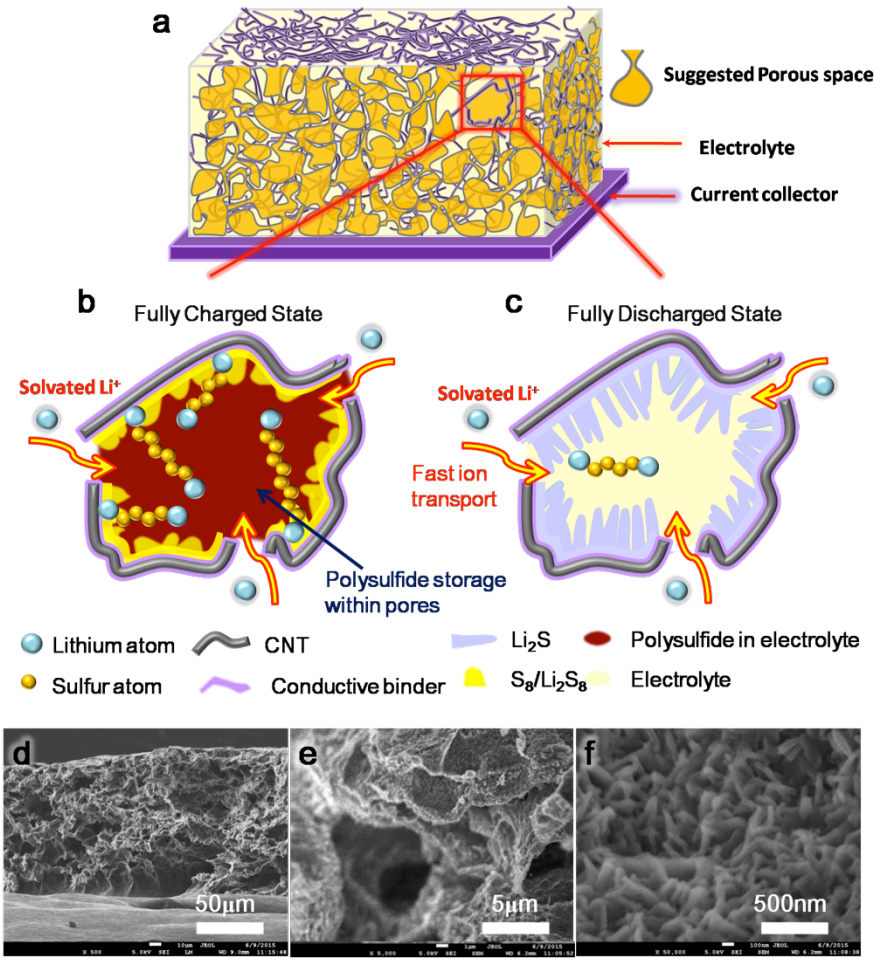

Figure 4. Schematic diagram of the CNT-nest-S electrode structure (a) and a local magnification diagram in fully charged (b) and discharge state (c) to illustrate the working mechanism of the nest structure. (d-f) SEM images of the cross-section morphology of the CNT-nest-S electrode with 3mgcm^{-2} sulfur loading, discharged at C/3 after two C/10 cycles.

Working mechanism analysis of the ant-nest Li-S electrode. The high performance of the CNT-nest-S Li-S cells stems from the unique property of the nest structure. The working mechanism of the nest structure is demonstrated in the diagram in Fig. 4(a-c), and the electrode structures via post-mortem analysis in Fig. 4(d-f). Several key mechanisms are of interest. First, the interconnected channels for ion transport are highly efficient in assisting ultrafast reaction dynamics. Numerous interconnected channels between porous structures are created

spontaneously during the sacrificial fabrication process, penetrating throughout the electrode. They remain unblocked even after fast discharge in high loading Li-S cells, shown in Fig. 4(d-e) in the zoom-in cross-section SEM morphology. Therefore, the blocking issue that has traditionally occurred in high loading Li-S cells is successfully overcome. Secondly, ample pore structure exists as storage space throughout the electrode. This storage space can easily sustain the dissolved polysulfide in the porous structure, as shown in Fig. 4(d). The polysulfide is kept from diffusing into the open electrolyte, minimizing the shuttle effect. Also, the affinity between the polysulfide and the functionalized binder can improve the storage efficiency. The clear color of electrolyte on the separator from the dissembled cell at fully discharged state shows this reduced effect, shown in the inset of Fig. 3(a), when comparing with the color of the electrolyte in the CNT-S cell shown in Fig. 1(b). Thirdly, the conductive binder can help to improve electrode conductivity, and the porous structure with the large surface area of CNT helps to extend the reaction surface area. Therefore, an efficient transformation of the sulfur species is observed during the charge (S_8/Li_2S_8) and discharge process (Li_2S/Li_2S_2), demonstrated in Fig. 4(b-c), and is also proved by the clear electrolyte in the inset of Fig. 3(a). This research demonstrates—via the good performance of high loading Li-S cells—the effectiveness of an efficient Li-S electrode that mimics the beauty of an ant-nest structure.

Difference in the morphology of the sulfur species in the fully charged state (S_8/Li_2S_8) and discharged state (Li_2S/Li_2S_2) is depicted in Fig. 4(b) and (c). The semi-transparent yellow region with the blurred edge refers to the elemental sulfur (S_8), or the long chain polysulfide (Li_2S_8)[32-34].. The needle-shaped structure is drawn in Fig. 4(c) to depict the morphology of Li_2S/Li_2S_2. An interesting morphology of the needle-shaped structure is observed inside the micro-pores at fully discharged state in CNT-nest-S electrode, with high magnification SEM in Fig. 4(f). All of the

inner walls inside the pores are covered by the needle-shaped structure, which is smaller than 50nm in diameter and approximately 200 nm in length. Since a large relative ratio of sulfur is observed by EDX, and a capacity of more than 900 $mAhcm^{-2}$ is obtained, the needle-shaped sulfur species can be assigned to be Li_2S in this fully discharged state. It is interesting that the needle structure is very sensitive to electron beam irradiation. Fig. S3(a-i) show the SEM images taken continuously on the same spot in Fig. S4(a). The needle-shaped structure will gradually evaporate away after continuous expose to electron beam in SEM, and only bare CNT framework, underlying the needle-shaped structure, will be left. Although not thoroughly reported in other research, this needle-shaped structure could possibly be Li_2S nanowires grown on the CNT surface. Analogous to the nanowire growth in other inorganic systems, the needle-shaped structures are guessed to be the result of surface tension, discontinuous crystal structure growth in initial atom layers, and the subsequent precipitation[35,36]. The extended high conductive surface area of the electrode decreases the current density; therefore, it promotes growth of the Li_2S crystal along its preferred crystal direction[37,38]. In comparison, blanket-shaped Li_2S covers the whole surface area of CNT-S; no nanostructure is observed on the surface, as shown in the inset of Fig. 1(a). The ant-nest structure of the CNT-nest-S electrode has more assessable electrode surface area for S species precipitation. Therefore, the current density is much lower throughout the CNT-nest-S electrode, kinetically favoring the directional Li_2S crystal growth rather than homogenous blanket precipitation. Furthermore, the needle-shaped Li_2S has less blocking effect to the lithium ions transport in CNT-nest-S, than to the blanket coverage in CNT-S. This further shows the positive effect of CNT-nest-S electrodes in assisting polysulfide precipitation with the enlarged, high-conductive surface and unblocked ion transport pathway.

The characteristics of the ant-nest structure are further demonstrated in the detailed comparison between the CNT-nest-S and regular CNT-S. When fast discharge is applied on the high loading CNT-S cells, the sulfur species precipitates on the surface of the electrode and blocks channels from further reaction, as shown in the Fig. 1(a) inset. A large quantity of bare CNT network is observed in TEM with a very small amount of observable Li_2S precipitation, shown in Fig. S4 (a, b). On the CNT-nest-S, the edges of the entire surface are covered by Li_2S precipitation, clearly showing the CNT network, and with small random pores still visible (shown in Fig. S4(c, d)). This difference in sulfur distribution is also observed in EDX mapping. Very little sulfur content and high carbon levels are detected in the regular CNT-S electrode, shown in Fig. S5 (a-c), while more sulfur content is detected all over the scan area in the CNT-nest-S electrode, with less carbon detected, shown in Fig. S5 (d-f). A larger relative quantity of the sulfur to carbon content is observed in CNT-nest-S with EDX. In CNT-nest-S, the relative S to C ratio is 0.38, which is 19 times higher than in the regular CNT-S electrode.

High-sulfur-ratio Li-S batteries. Another major challenge addressed in this research is the low sulfur ratio of an Li-S electrode as applied in the current Li-S system—usually below 60wt% (to total electrode mass). As discussed frequently in recent research, the high fraction of non-active material decreases electrode level capacity, and significantly lowers the energy density of a Li-S battery[22,29], which is highly undesirable. Although several attempts have been made towards a higher sulfur ratio electrode, results have not been satisfactory[30]. The novel nest-structure electrode proposed in this work demonstrates good cycling and rate performance on high-loading Li-S batteries and its potential can be further achieved in ultra-high sulfur ratio (up to 85wt%) application.

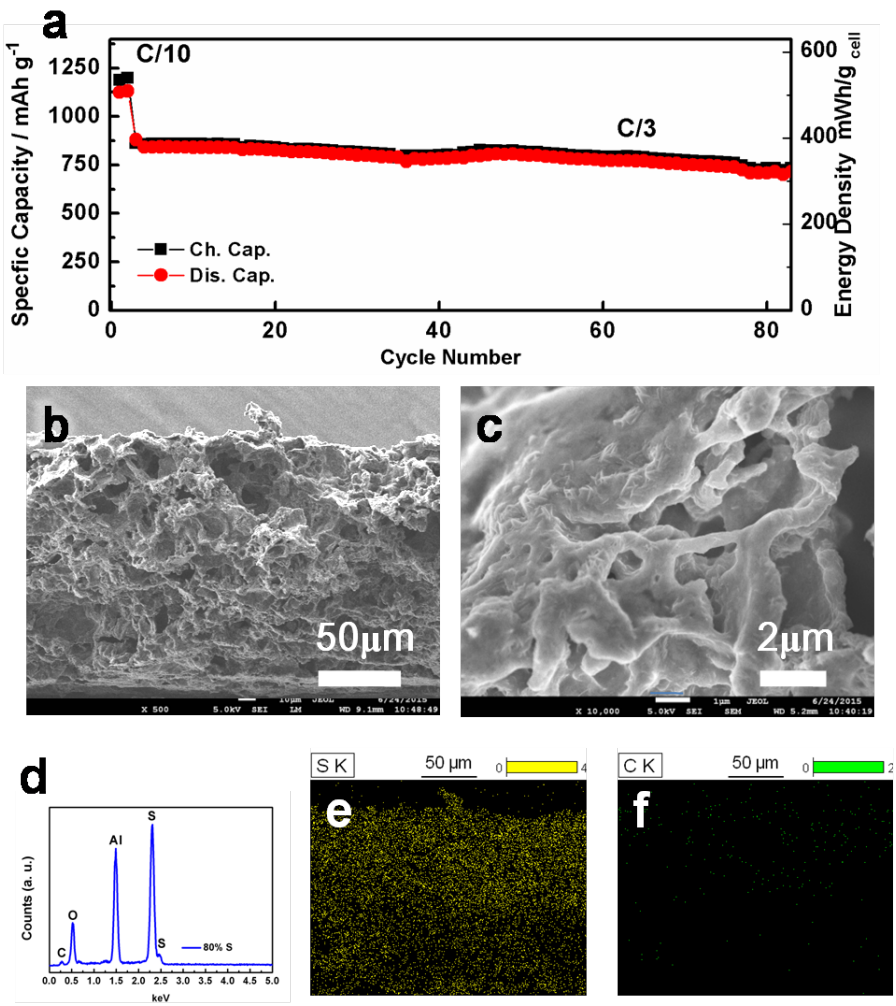

Figure 5.(a) Cycling performance of the 80%S-nest-S cell, both the sulfur-level specific capacity (left scale) and the cell-level Energy Density (right scale) are included. SEM images of cycled 80%S-nest-S electrodes cross-section morphology (b) and zoom-in morphology (c). EDX data (d) and EDX mappings (e, f) for the cycled 80% S-nest-S electrode corresponding to the area shown in (b).

The ant-nest structure's ability to allow for ultra-high sulfur ratio Li-S batteries is first demonstrated by the 80 wt% sulfur in composite electrode (named 80%S-nest-S), which is composed solely of 80 wt% sulfur, 5 wt% binder, and 15 wt% CNT. All cells have sulfur loading levels ranging from 2.5mg cm^{-2} to 3 mg cm^{-2}. The cycling performance is plotted in Fig. 5(a). A high capacity of 1123.5 $mAhg^{-1}$ is achieved at C/10 (167 mAg^{-1}) and 908.5 $mAhg^{-1}$ is obtained at C/3 (558 mAg^{-1}) for the 80%S-nest-S cell. Its energy density, based on cell level calculation, is

also plotted on the right scale of Fig. 5(a). The mass of each cell component for the energy density calculation is listed in Table S1. When the mass from the cell is calculated, energy density of the 80%S-nest-S cell is 509mWhg^{-1} at C/10 and 374mWh g^{-1} at C/3. The cell has achieved 2.8 and 2 times the level of state-of-the-art Li-ion batteries (180 Whkg^{-1})[22]. This value is attractive when compared to any other recent work. What's more, a high capacity of ~937 mAhg^{-1} can be achieved at C/10 (167 mAg^{-1}) for the 85%S-nest-S cell (85 wt% sulfur, 3 wt% binder, and 12 wt% CNT), with stable performance of 800 mAhg^{-1} over 80 cycles, shown in Fig. S6. In this way, the battery makes full use of the ant-nest structure and increases the sulfur loading at the same time—with significant decrease in the ratio of the non-active material.

To better understand the ant-nest structure mechanism with high sulfur loading and high sulfur ratio, post mortem analysis of the cycled cell is performed with 80%S-nest-S after two cycles at C/10 and discharge at C/3. Cross-section morphology of the 80%S-nest-S cell is observed through SEM in Fig. 5(b,c). As shown, the ant-nest structure remains, exhibiting large pores and un-blocked interconnected channels. A very thick Li_2S precipitation layer is observed coating the surface of the CNT network. This indicates that with the assistance of a highly conductive CNT network and conductive binder, the reaction surface is highly efficient for resistive Li_2S precipitation. Also, the numerous porous structures can provide enough space for a large quantity of polysulfide storage and a large surface for efficient precipitation. Noticeable shrinkage of the interconnected channels is observed, but they mostly remain open after the fast discharge; therefore, fast ion transport can be ensured in high loading Li-S cells. Further evidence of the superior capability in sulfur species (Li_2S) precipitation is given via EDX, shown in Fig. 5(d-f). A high relative sulfur to carbon content (S to C ratio: 1.88) is observed: 94 times the regular CNT-S and 5 times the 50%-CNT-nest-S. EDX mapping further demonstrates the high sulfur

composition ratio and full-coverage in the porous structure. The 80%S-nest-S is completely covered by sulfur species (Li_2S) with the CNT frame work buried beneath; large quantities of sulfur and carbon signal can hardly be detected, shown in Fig. 5 (e,f).

In this way, the unique properties of the ant-nest structure is clearly demonstrated via the hosting of ultra high sulfur ratio in high-loading Li-S batteries. The design idea of the ant-nest structure has been fulfilled: with large storage area and functionality to attract and sustain polysulfide, the multi interconnected channels to assist fast ion transportation, and the highly conductive CNT and conductive binder to ensure the high conductivity of the entire electrode. Further efforts are needed for over-all cell optimization.

Discussion

The novel, nature-derived ant-nest structure Li-S electrode has demonstrated the possibility of achieving electrode-scale production of high-loading, high-sulfur-ratio Li-S batteries that cost little to manufacture and use easy and manufacturing-friendly methods including slurry ball-milling, doctor-blade based laminate casting, and feasible sacrificial methods for creating a porous surface. The sacrificial method, using table salt as a method for creating the biomimetic ant-nest structure, is unique and effective, and bypasses some of the complicated and expensive materials or multi-step synthesis methods needed to solve the open issues[14]. By re-creating the superb, nature-designed, three-dimensional ant-nest structure using table salt, the Li-S electrode obtains the unique properties of the ant-nest structure. By bio-mimicking the smart spacial design of a porous ant-nest structure, and applying the inner surface decoration with a functional binder, efficient polysulfide suspension is achieved within the porous storage space and enhanced by the strong affinity between the functional binder and polysulfide. Also, the multi-interconnected

channels of the ant-nest structure are created spontaneously in the sacrificial synthesis process, which endows ultra fast ion transport capability to the Li-S electrode. The extended inner surface via the porous ant-nest structure provides an extra-large reaction interface for polysulfide transformation and precipitation. The conductive binder, along with the highly conductive carbon nanotube, helps to enhance the conductivity of the reaction interface and long-distance charge transport.

Porous structures are created in two scales: micro- and nano-scale. The nano-scale refers to the space between single nanotubes, which scatter around the micro-pores and can enable use of the entire large carbon nanotube surface. This marvelous ant-nest structure has shown strong capability in carrying high sulfur loading, and can increase the sulfur ratio as high as 85%, with only 12% CNT and 3% conductive binder, which is the same composition of active material as the commercial cathode. The 85% sulfur electrode can not only sustain the mechanical force during polysulfide dissolution and precipitation but also can provide all the necessities for the reaction of high loading Li-S batteries, as discussed above. Both good cycling/rate performance and high sulfur utilization is achieved in this novel, high-loading sulfur electrode, which suggests that the efficient spacial design of the Li-S electrode is indeed the solution to achieving high loading industrialized Li-S batteries.

Further research is still needed to explore the potential of this ant-nest structure. Since the ant-nest structure Li-S electrode is designed with sacrificial household table salt, further research could optimize the micro-pore through size and distribution control of the sacrificial table salt. Also, improved use of the ultra large surface of the carbon nanotube (nano-pores between each nanotube) can be achieved via further control of the solvent evaporation process during doctor-blade laminate casting. Furthermore, in order to improve the stability of the high-loading Li-S

batteries, the optimization of the electrolyte composition, and protection of lithium counter electrode should be further studied, via surface protection[39] or addition of additives[14], etc.

In conclusion, this research shows the viability of an electrode-scale nature-inspired ant-nest structure electrode for the application of high loading Li-S batteries. It processes the unique properties of the ant-nest structure of the large polysulfide storage capability and highly efficient, multi interconnected ion transportation pathway design and extended reaction interface to achieve unique direction crystalline S species precipitation on the surface of the CNT.

Methods

Materials

The sulfur powder is purchased from U.S. Research Nanomaterials, Inc. CNT and NaCl is purchased from Sigma-Aldrich Inc. Poly(9,9-dioctylfluorene-co-fluorenone-co-methylbenzoic ester)(PFM) is synthesized according to previous work[40]. The chlorobenzene (Sigma-Aldrich Inc.) is used as the solvent for PFM. The electrolyte for cell testing is composed of 1 M lithium salt bis(trifluoromethanesulfonyl)imide (LiTFSI) dissolved in 1,3-dioxolane/1,2-dimethoxyethane/(n-methyl-(n-butyl) pyrrolidiniumbis(trifluoromethanesulfonyl)imide DOL/DME/PyR14TSFI (3:3:2 in volume), and 1 wt% LiNO3, all purchased from Sigma-Aldrich.

Cathode fabrication

The PFM is dissolved in chlorobenzene at 5 wt% ratio. Sulfur powder and CNT are added into the binder-solvent solution after the binder is dissolved. For the regular electrode, the weight ratio of these three components is: 50% sulfur, 10% PFM, 40% CNT. The NaCl particles are first ball-milled into micro-sized particles and then added to the slurry for the nest structure electrode. The composition of the nest structure electrode is 50% sulfur 10% PFM, 40% CNT for the 50%S

electrode; 80% sulfur, 4% PFM, 16% CNT for the 80%S electrode; and 85% sulfur, 3% PFM, 12% CNT for the 85%S electrode. The mixture is combined using the ball-milling method overnight to obtain uniform slurry. The laminate is then made by coating the slurry on a 30-μm-thick battery-grade nickel current collector with a Mitutoyo doctor blade and an Elcometer motorized film applicator. Mass loading of sulfur is 1.5-3 mg cm^{-2}. After the laminate is fully dried, it is further dried in a vacuum oven at 50 °C overnight.

Cell assembly and testing

Li-S batteries are tested with 2325-type coin cells (National Research Council Canada). The cells are assembled in an argon-filled glove box with oxygen content less than 0.1 ppm. The size of the sulfur electrode is 1/2-inch OD, and the size of the counter electrode lithium metal disk is 11/16-inch OD. The Li foil is purchased from FMC-Lithium Co. The separator used is polypropylene film (Celgar 2400). Galvanostatic cycling tests are performed on a Maccor series 4000 cell tester (Maccor, Inc., Tulsa, OK). The voltage window for cell test is 1.7–2.7 V. The cells are cycled at C/10 for 2 cycles before any other test.

Material characterization techniques

Morphology of the electrode surface is characterized with a JSM-7500F scanning electron microscope at the National Center for Electron Microscopy (NCEM) at Lawrence Berkeley National Laboratory. An energy dispersive X-ray (EDX) spectrometer attached to the SEM (JEOL JSM-7500F) was used to conduct elemental analysis of sulfur and the distribution with an accelerating voltage of 15 kV. Transmission Electron Microscopy (TEM) images was produced by a 200 kilovolt FEI monochromated F20 UT Tecnai. Thermo gravimetric analysis (TGA, TA

Instruments Q5000) was used to determine the ratio of the S in the electrode using a heating rate of 10℃/min in N_2.The cycled Li-S batteries are opened with a cell opener for post-test analysis, and the electrode is washed thoroughly with DOL/DME with a volume ratio of 1:1 inside an argon-filled glove box.

Acknowledgements

This work is funded by the Assistant Secretary for Energy Efficiency, Office of Vehicle Technologies of the U.S. Department of Energy (U.S. DOE) under the Advanced Battery Materials Research (BMR) program, along with the National Center for Electron Microscopy of the Molecular Foundry and the Advanced Light Source at the Lawrence Berkeley National Laboratory, which are supported by the U.S. Department of Energy under Contract # DE-AC02-05 CH11231. Guo Ai and Wenfeng Mao are supported by the China Scholarship Council.

Author contributions

G. A., Y. D., H. Z. and G. L. conceived the idea, designed experiments and analyzed the data. G. G.A. and W. M. carried out the synthesis of materials and electrochemical tests. G. A., W. M. and X. S. performed the characterization of materials. Y. F., Y. E., V. B., V.S. and G. L. contributed to the discussion of the results. G. A. and G. L. co-wrote the paper. All the authors commented on and revised the manuscript.

1 Tarascon, J. M. & Armand, M. Issues and challenges facing rechargeable lithium batteries. *Nature* **414**, 359-367 (2001).

2 Cho, J., Jeong, S. & Kim, Y. Commercial and research battery technologies for electrical energy storage applications. *Progress in Energy and Combustion Science* **48**, 84-101, doi:10.1016/j.pecs.2015.01.002 (2015).

3 Goodenough, J. B. & Kim, Y. Challenges for Rechargeable Li Batteries. *Chemistry of Materials* **22**, 587-603, doi:10.1021/cm901452z (2010).

4 <Nature-A BETTER BATTERY.pdf>.

5 Barghamadi, M., Kapoor, A. & Wen, C. A Review on Li-S Batteries as a High Efficiency Rechargeable Lithium Battery. *Journal of the Electrochemical Society* **160**, A1256-A1263, doi:10.1149/2.096308jes (2013).

6 Bresser, D., Passerini, S. & Scrosati, B. Recent progress and remaining challenges in sulfur-based lithium secondary batteries – a review. *Chemical Communications* **49**, 10545, doi:10.1039/c3cc46131a (2013).

7 Bruce, P. G., Freunberger, S. A., Hardwick, L. J. & Tarascon, J.-M. Li–O2 and Li–S batteries with high energy storage. *Nature Materials* **11**, 19-29, doi:10.1038/nmat3191 (2011).

8 Chen, L. & Shaw, L. L. Recent advances in lithium–sulfur batteries. *Journal of Power Sources* **267**, 770-783, doi:10.1016/j.jpowsour.2014.05.111 (2014).

9 Evers, S., Yim, T. & Nazar, L. F. Understanding the Nature of Absorption/Adsorption in Nanoporous Polysulfide Sorbents for the Li–S Battery. *The Journal of Physical Chemistry C* **116**, 19653-19658, doi:10.1021/jp304380j (2012).

10 Song, J. *et al.* Strong Lithium Polysulfide Chemisorption on Electroactive Sites of Nitrogen-Doped Carbon Composites For High-Performance Lithium–Sulfur Battery Cathodes. *Angewandte Chemie International Edition*, n/a-n/a, doi:10.1002/anie.201411109 (2015).

11 Mikhaylik, Y. V. & Akridge, J. R. Polysulfide Shuttle Study in the Li/S Battery System. *Journal of The Electrochemical Society* **151**, A1969, doi:10.1149/1.1806394 (2004).

12 Chen, H. *et al.* Ultrafine Sulfur Nanoparticles in Conducting Polymer Shell as Cathode Materials for High Performance Lithium/Sulfur Batteries. *Scientific Reports* **3**, doi:10.1038/srep01910 (2013).

13 Wei Seh, Z. *et al.* Sulphur–TiO2 yolk–shell nanoarchitecture with internal void space for long-cycle lithium–sulphur batteries. *Nature Communications* **4**, 1331, doi:10.1038/ncomms2327 (2013).

14 Yao, H. *et al.* Improving lithium–sulphur batteries through spatial control of sulphur species deposition on a hybrid electrode surface. *Nature Communications* **5**, doi:10.1038/ncomms4943 (2014).

15 Song, J. *et al.* Nitrogen-Doped Mesoporous Carbon Promoted Chemical Adsorption of Sulfur and Fabrication of High-Areal-Capacity Sulfur Cathode with Exceptional Cycling Stability for Lithium-Sulfur Batteries. *Advanced Functional Materials* **24**, 1243-1250, doi:10.1002/adfm.201302631 (2014).

16 Pang, Q., Kundu, D., Cuisinier, M. & Nazar, L. F. Surface-enhanced redox chemistry of polysulphides on a metallic and polar host for lithium-sulphur batteries. *Nature Communications* **5**, 4759, doi:10.1038/ncomms5759 (2014).

17 Seh, Z. W. *et al.* Stable cycling of lithium sulfide cathodes through strong affinity with a bifunctional binder. *Chemical Science* **4**, 3673, doi:10.1039/c3sc51476e (2013).

18 Ai, G. *et al.* Investigation of surface effects through the application of the functional binders in lithium sulfur batteries. *Nano Energy* **16**, 28-37, doi: http://dx.doi.org/10.1016/j.nanoen.2015.05.036 (2015).

19 Gordin, M. L. *et al.* Bis(2,2,2-trifluoroethyl) Ether As an Electrolyte Co-solvent for Mitigating Self-Discharge in Lithium–Sulfur Batteries. *ACS Applied Materials & Interfaces* **6**, 8006-8010, doi:10.1021/am501665s (2014).

20 Scheers, J., Fantini, S. & Johansson, P. A review of electrolytes for lithium–sulphur batteries. *Journal of Power Sources* **255**, 204-218, doi: http://dx.doi.org/10.1016/j.jpowsour.2014.01.023 (2014).

21 Yang, Y., Zheng, G. & Cui, Y. Nanostructured sulfur cathodes. *Chemical Society Reviews* **42**, 3018, doi:10.1039/c2cs35256g (2013).

22 Lv, D. *et al.* High Energy Density Lithium-Sulfur Batteries: Challenges of Thick Sulfur Cathodes. *Advanced Energy Materials*, n/a-n/a, doi:10.1002/aenm.201402290 (2015).
23 Yang, Y. *et al.* High-Capacity Micrometer-Sized Li2S Particles as Cathode Materials for Advanced Rechargeable Lithium-Ion Batteries. *Journal of the American Chemical Society* **134**, 15387-15394, doi:10.1021/ja3052206 (2012).
24 Wang, Q. *et al.* Improve Rate Capability of the Sulfur Cathode Using a Gelatin Binder. *Journal of The Electrochemical Society* **158**, A775-A779, doi:10.1149/1.3583375 (2011).
25 Barchasz, C. *et al.* Novel positive electrode architecture for rechargeable lithium/sulfur batteries. *Journal of Power Sources* **211**, 19-26, doi:http://dx.doi.org/10.1016/j.jpowsour.2012.03.062 (2012).
26 Cheon, S.E. *et al.* Rechargeable Lithium Sulfur Battery: II. Rate Capability and Cycle Characteristics. *Journal of The Electrochemical Society* **150**, A800-A805, doi:10.1149/1.1571533 (2003).
27 Latty, T. *et al.* Structure and formation of ant transportation networks. *Journal of The Royal Society Interface* **8**, 1298-1306, doi:10.1098/rsif.2010.0612 (2011).
28 <Nano Lett. 2008 Zhang.pdf>.
29 Zhou, G. *et al.* A graphene foam electrode with high sulfur loading for flexible and high energy Li-S batteries. *Nano Energy* **11**, 356-365, doi:10.1016/j.nanoen.2014.11.025 (2015).
30 <Long-life Lipolysulphide batteries with.pdf>. doi: 10.1038/ncomms8760|www.nature.com/naturecommunications.
31 <yicui_ppt.pdf>.
32 <Hu_et_al-Advanced_Materials.pdf>. doi:10.1002/adma.201504765.
33 <JPS-90S-A proof-of-concept lithium sulfur liquid battery with exceptionally high capacity.pdf>. doi:10.1016/j.jpowsour.2012.04.006.
34 <Moon_et_al-2013-Advanced_Materials.pdf>. doi:10.1002/adma.201303166.
35 <srep14949.pdf>. doi:10.1038/srep14949.
36 <TOMSJ-5-215.pdf>.
37 <srep04629.pdf>. doi:10.1038/srep04629.
38 <Li-S Battery Analyzed by UV Vis in Operando Mode.pdf>. doi:10.1002/cssc.201300142.
39 <New insight into the working mechanism of lithium–sulfur batteries in situ and operando X-ray diffraction characterization.pdf>. doi:10.1039/c3cc43766c.
40 Liu, G. *et al.* Polymers with Tailored Electronic Structure for High Capacity Lithium Battery Electrodes. *Advanced Materials* **23**, 4679-4683, doi:10.1002/adma.201102421 (2011).